

MODELLING OF MULTICOMPONENT SANDY BEDS EVOLUTION  
UNDER SHALLOW WATER WAVES

G. Chapalain<sup>1</sup> and B. Boczar-Karakiewicz<sup>2</sup>

ABSTRACT

A study of hydrodynamics and multicomponent sedimentary processes associated to unbroken water waves propagating in coastal areas is presented. For the specific case in which the waves are normally incident, weakly non-linear and dispersive, and the foreshore profile displayed a gentle slope, a model of wave-induced heterogeneous sand transport and resulting topographical and granulometric changes is developed. The general conclusion of this study is that the model presented describes some of the observed features of the sedimentology of longshore bars systems.

INTRODUCTION

Coexistence of several classes of sediments of varying sizes is a striking characteristic of coastal environments. This is due to the fact that the vectors for the sediment, i.e. rivers, transport granulates of various sizes. Coastal hydrodynamic forces subsequently redistribute the sediment within the medium. In the foreshore areas where sandbar systems develop, descriptive investigations (Sitarz, 1963; Davis and McGreary, 1965; Fox et al., 1966; Bajorunas and Duane, 1967; Mothersill, 1969; Saylor and Hands, 1970; Long et al., 1984; Forbes et al., 1986) have shown a high correlation between granulometry and bathymetry (Figures 1-2). The majority of observations reveals a localization of coarse fractions ( $0 < \phi < 2$ ) in the troughs and fine grain fractions ( $2 < \phi < 3$ ) at the crests. Moreover, the majority of observations shows that better sorted sediments are located at the crests and poorly sorted sediments are located in the troughs.

Various mechanisms have been invoked to account of the development of nearshore multiple longshore sand bars. These have included standing waves (Carter et al., 1973), edge-waves (Bowen and Inman, 1971), undertow and rip-cell circulation (Dyhr-Nielsen and Sorensen, 1970) and the non-linear interaction of higher harmonics in a regular incident wavetrain during shoaling (Boczar-Karakiewicz et al., 1981).

In the present paper, we focusse on the outer part of gently sloping profiles and therefore concentrate on the last mechanism which involves the non-linear evolution of progressive waves as they approach the shore. To proceed in an idealized way a two dimensional situation wherein a deepwater plane periodic wavetrain impinges on the shore is considered. It is assumed that the activity of edge-waves and breaking waves is reduced or confined close to the shore.

The model is composed of four constituents, describing processes involved in the mechanism of wave-bed interactions: (1) the surface hydrodynamics, (2) the near-bed boundary layer flow, (3) the sediment transport, and (4) the evolution of the bottom topography and composition. All four modules are linked together in a two-step morphological time-loop. In the first step, the fluid flow and the heterogeneous sediment flux are calculated over a bed configuration which is instantaneously fixed. In the second step, the temporal evolution of the seabed is calculated while keeping all variables describing the fluid and sediment flow constant. The two-step approximation is justified by observations in laboratory and in natural coastal environments (Boczar-Karakiewicz et al., 1987; Boczar-Karakiewicz and Davidson-Arnott, 1987)

---

<sup>1</sup> Institut de Mécanique de Grenoble, BP53X, 38041 Grenoble, France

<sup>2</sup> INRS-Océanologie, Université du Québec, 310 ave. des Ursulines, Rimouski, PQ, Canada

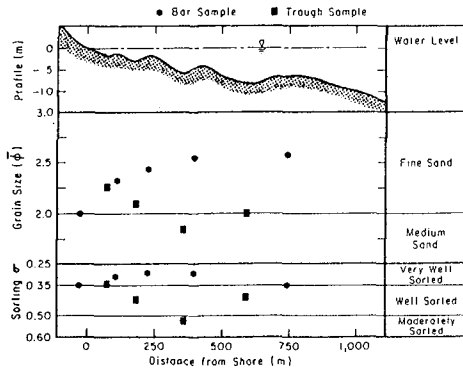


Figure 1. Measurements of mean value  $\bar{\phi}$  and of the sorting  $\sigma$  across bar systems in Great Lakes (Saylor and Hands, 1970).

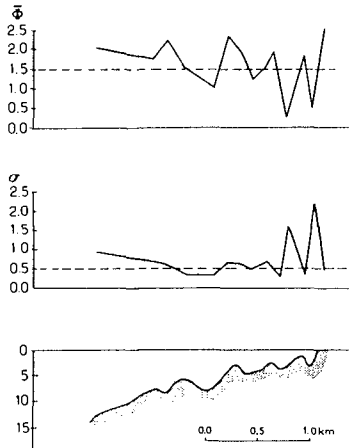


Figure 2. Spatial structures of the mean value  $\bar{\phi}$  and of the sorting  $\sigma$  across a bar system on the north shore of the St Lawrence estuary (Long et al., 1984).

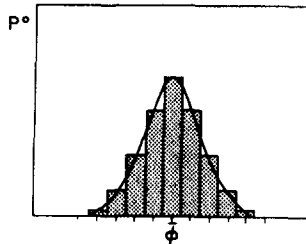


Figure 3. Initial granulometric distribution.

WAVE FIELD DESCRIPTION

The incident regular two-dimensional wavetrain is characterized by an amplitude  $a$  and a wavelength  $L$ . It propagates in a domain described by a coordinate system  $(x, z)$ . The undisturbed water level is at  $z = 0$  and  $h(x)$  is the water depth at point  $x$ . The vertical deviation from equilibrium of the free surface at point  $x$  at time  $t$  is  $\xi(x,t)$  and  $q(x,t)$  is the depth-averaged horizontal velocity. All physical variables are non-dimensionalized and scaled:

$$h = \frac{\bar{h}}{H}, \quad x = \frac{\bar{x}}{H}, \quad t = \frac{\bar{t}}{\sqrt{H/g}}, \quad \xi = \frac{\bar{\xi}}{\alpha H}, \quad q = \frac{\bar{q}}{\alpha \sqrt{gH}} \tag{1}$$

where  $H$  represents a characteristic depth,  $g$  is the acceleration due to gravity,  $\alpha = a/H$  is a relative wave amplitude parameter.

The Boussinesq set of equations describing the shallow water wave is modified by a dissipative term induced by the bottom shear stress of the underlying turbulent boundary layer:

$$q_t + \xi_x + \alpha q q_x = \frac{h^2}{3} q_{xx} + h h_x q_{xt} + \frac{1}{2} h h_{xx} q_t + \frac{R}{h} q \tag{2}$$

$$\xi_t + [(\alpha \xi + h) q]_x = 0 \tag{3}$$

In the derivation of the dissipative term  $(R/h)q$  it has been assumed that friction is linear, where the constant  $R = 3/4 \pi f_w \alpha q_{max}$  is expressed by constant flow and friction parameters: the depth-averaged maximum velocity  $q_{max}$  at  $x = 0$ , and Jonsson's (1978) friction coefficient  $f_w$

$$\left\{ \begin{array}{ll} f_w = \frac{0.0605}{\text{Log}^2 \frac{27\delta_1}{k_b}} & k_b/a_b < 1 \\ f_w = 0.24 & k_b/a_b > 1 \end{array} \right. \tag{4}$$

where  $\delta_1$ ,  $k_b$  and  $a_b$  are respectively the Jonsson's length, the roughness height and half of the near-bed orbital excursion (see Grant and Madsen, 1982).

Following Lau and Barcelona (1972) and Boczar-Karakiewicz et al (1987) we are seeking for a solution of (2) and (3) where the free surface elevation  $\xi$  is presented by a simple modal decomposition

$$\xi = \xi(x,X,t) = \sum_{j=1}^2 a_j(X) \exp [i (k'_j x - \omega_j t)] + c.c. \tag{5}$$

The first-order amplitudes  $a_j$  in (5) are taken to vary on the scale of wavelengths, and therefore depend on  $X$  which is a horizontal length-scale measured in wavelength  $L$  (i.e.  $X = \bar{x}/L = \beta x$  where  $\beta = H/L$  is the aspect ratio for the motion assumed to be of the order of  $\alpha$ ). In equation (5) c.c. stands for the complex conjugate of the quantity just preceding it. A similar representation is postulated for  $q$ .

In (5)  $\omega_1$  is the frequency of the postulated incoming wavetrain, and  $\omega_2 = 2\omega_1$  is its second harmonic,  $k'_1$  and  $k'_2$  are wave numbers associated with  $\omega_1$  and  $\omega_2$  respectively.

It is further assumed that the principal features of the bottom variation are gradual, and therefore, it also may be taken that  $h$  is a function  $h(X)$  (i.e.  $h(X) = 1 + O(\alpha)f(X)$  where  $f$  is an  $O(1)$  function) of the long variable, only.

The dispersion relation results from linear theory (first-order) and reads

$$k_j'^2 = k_j^2 + i \frac{R \omega_j}{1 - \frac{\omega_j^2}{3}} \quad (6)$$

where  $k_j$  denotes the first-order wave numbers obtained when friction is ignored.

The amplitudes  $\xi_j$ , and consequently of the depth-averaged velocities  $q$  result from solvability conditions for the second-order approximation (Lau and Barcilon, 1972)

$$\begin{cases} a_1 X + H_1(X) a_1 + S_1(X) \exp\left(\frac{\Delta k^I X}{\beta}\right) \exp\left(-i \frac{\Delta k^R X}{\beta}\right) a_1 a_2^* = 0 \\ a_2 X + H_2(X) a_2 + S_2(X) \exp\left(\frac{\Delta k^I X}{\beta}\right) \exp\left(i \frac{\Delta k^R X}{\beta}\right) a_2^2 = 0 \end{cases} \quad (7)$$

where \* denotes complex conjugation,  $\Delta k' = \Delta k^I + i \Delta k^R = k_2' - 2k_1'$ ,  $H_1$ ,  $H_2$ ,  $S_1$  and  $S_2$  are known functions of  $X$ .

As shown in (6) and (7), the essential modifications induced by a linear friction term appear in the first-order dispersion relation (6). The non-linear equations (7) for the amplitudes  $a_j$  ( $j = 1, 2$ ) remain identical when compared to the frictionless model (see Lau and Barcilon, 1972; Boczar-Karakiewicz et al., 1987), except that in all coefficients the frictionless wave-number  $k_j$  has to be replaced by  $k_j'$ .

For a chosen frequency  $\omega_1$  of the incident wave the set of equations (7) has to be completed by the initial values at  $X = 0$ :

$$a_1(0) = 1; \quad a_2(0) = 0 \quad (8)$$

reflecting the assumption that the incoming regime is composed of a single-frequency wavetrain.

The coupled system of non-linear evolution equations (7) supplemented by (8) are solved numerically using a stable and accurate fourth-order Runge-Kutta method.

### WAVE-INDUCED NEAR-BED BOUNDARY LAYER PROCESSES

The governing equations for the near-bottom flow with suspended sediment are simplified by several assumptions. It is assumed that

- the suspended sediment concentration is sufficiently low to neglect particle interactions, but high enough to represent the mixture as a continuum,
- the fluid is newtonian,
- the inertia of the particles is assumed to be small and thus the sediment velocity is equal to the fluid velocity minus the particle fall velocity.

Completing the previous assumptions by Boussinesq's formulation of the Reynolds shear stress and the turbulent mass flux, the sediment-laden flow may be approximately described by the following system of equations

$$\frac{\partial u}{\partial t} = -\frac{1}{\rho_f} \frac{\partial p}{\partial x} + \frac{\partial}{\partial z} \left( \gamma_t \frac{\partial u}{\partial z} \right) \quad (9)$$

$$\frac{\partial c(K)}{\partial t} = w_f(K) \frac{\partial c(K)}{\partial z} + \frac{\partial}{\partial z} \left( \gamma_t(K) \frac{\partial c(K)}{\partial z} \right) \quad (10)$$

$$\rho = \rho_s C + (1-C) \rho_f, \quad C = \sum_{K=1}^{KM} c(K) \quad (11)$$

where  $u$  denotes the horizontal fluid velocity inside the boundary layer,  $p$  is the pressure,  $c(K)$  is the volumetric concentration of suspended sediment of class  $K$ ,  $KM$  is the number of classes,  $\rho$  is the density of the fluid-sediment mixture with  $\rho_f$  and  $\rho_s (= 2.65)$  denoting respectively the fluid and sediment density,  $\nu_t$  and  $\gamma_t(K)$  are respectively the eddy viscosity and diffusivity of sediment of class  $K$  and  $w_f(K)$  is the sediment fall velocity which can be determined as a function of the radius  $r(K)$  of the sediment particles of class  $K$  by the Gibbs et al.'s (1971)

$$w_f(K) = \frac{-3\mu_f + \sqrt{9\mu_f^2 + g r(K)^2 \rho_f (\rho_s - \rho_f) (0.015476 + 0.19841 \cdot r(K))}}{\rho_f (0.011607 + 0.14881 r(K))} \quad (12)$$

(Notice that all the physical quantities are expressed in c.g.s. units and  $\mu_f$  is the fluid dynamic viscosity).

The closure of the set of equations (9), (10), and (11) can be achieved at different levels of sophistication. For example a local "quasi-equilibrium" second-order closure is achieved by adding analytical expressions for the eddy viscosity  $\nu_t$  and for the eddy diffusivity  $\gamma_t$  and two transport equations for the turbulent macroscale  $\Lambda$  and the turbulent kinetic energy  $q^2$  (Sheng and Villaret, 1989).

Boundary conditions at the upper and lower limit of the boundary layer must be satisfied.

At the upper limit of the boundary layer it is required

(i) the mean horizontal velocities  $u$  to match the free stream velocity  $U_b$  (at  $z = -h$ ) of the main water body,

$$u = U_b = \frac{\alpha}{2} \left\{ \sum_{j=1}^2 \left( 1 - \frac{\beta^2 h^2 k_j^2}{6} \right) \left( -\frac{\omega_j}{k_j} \right) a_j(X) \exp \left[ i(k_j x - \omega_j t) \right] + c.c. \right\} \quad (13)$$

(ii) the vanishing of all turbulence-related characteristics and suspended sediment concentration.

At the lower limit of the boundary layer it is required

(i) to provide a near-bed mean velocity condition,

(ii) to provide a turbulent macroscale length model,

(iii) the vanishing of the turbulent energy flux,

(iv) to estimate the near-bed flux of sediment particles into the suspension. Numerous fluorescent or radioactive tracer measurements have revealed the existence of mixture in the topmost sediments. Conceptually, this mixing layer lends support to the idea of modelling the bottom by a juxtaposition of elementary boxes, whose vertical dimension will henceforth be related to the depth of the shifted sand. This thickness is correlated with the local hydrodynamic conditions and therefore the characteristics of boxes should vary in space. Given the limitations of the global modelling procedure, however, it will be assumed that the number of particles contained in an elementary box remains constant. In an erosion zone the problem arises of replacing the sediment removed from the control volume. One possibility consists of refilling with underlying sediment of the initial composition. This procedure, however, tends to drive the granulometric distribution back to the initial distribution, which ought in principle to be "forgotten" as the calculation proceeds, i.e. with increasing time. There is another alternative for the approach of equilibrium. Replacement can be achieved with sediment whose characteristics are identical with those calculated at the current time step, i.e. with a number of particles slightly smaller to the INP (hereinafter referred to as INP) in each box. In the initial stage, i.e. on an undeformed bed, it is assumed that the spatial composition of the sediment substrate is uniform throughout. The population of each class present is taken to be represented by a normal distribution. It will be denoted  $P^0(K)$ , where  $K$  designates the class. This weight frequency distribution is characterized by its mean value  $\phi^0$  and its standard deviation  $\sigma^0$ . The number of classes is fixed at nine with a  $\phi$ -interval equal to  $1/2$  (Figure 3). This distribution law was

selected because it represents the granulometric response to random hydrodynamic processes. The Initial Number of Particles in each class is then given by

$$N^0(K) = INP \cdot P^0(K) \quad (15)$$

The consequence of the superficial mixed layer concept on the near-bed flux of sediment particles into the suspension is an hypothesis of independence between the different fractions during the process of extraction and suspension of particles from the bed. Consequently, the near-bed sediment flux for each class  $K$  can be modelled by the Svendsen's (1977) pick-up function characterized by two peaks located at the free velocity reverses (i.e., phases when the vortices are released in the bottom boundary layer) and expressed as

$$p(K,t) = p_d(K) + \frac{p_d(K)}{1 + \mu} \sum_{n=1}^m \frac{2(m!)^2}{(m+n)! (m-n)!} \left\{ \cos n(\omega t - \varphi^+) + \mu \cos n(\omega t - \varphi^-) \right\} \quad (14)$$

where the parameter  $\mu = (U_b^-)^2 / [U_b^+]^2$  allows an account of non-linearities of the wave field. In (14)  $m$  is a parameter controlling the skewness of the peaks, superscripts  $+$  and  $-$  refer to the phases ( $\varphi^+$ ,  $\varphi^-$ ) of the velocity reverse following respectively the maximum and the minimum outer flow velocity; the quantity denoted by  $p_o(K)$  is equal to  $\bar{C}_0(K) \cdot w_f(K)$  where  $\bar{C}_0(K)$  is the mean bottom concentration is given by Nielsen (1979) as

$$\bar{C}_0(K) = 0.028 \left( \psi'(K) - \psi'_c(K) \right) \frac{2}{\pi} - \arccos \left( \frac{\psi'_c(K)}{\psi'(K)} \right)^{1/2} \quad (15)$$

with  $\psi'(K)$  and  $\psi'_c(K)$  are respectively Madsen and Grant's (1976) wave-extended Shields parameter and its critical value (Figure 4).

Conclusions resulting from numerical experiments using the coupled local "quasi-equilibrium" second-order turbulent closure model in single class version justify a simplification of the modelling procedure for a flow with a low sediment concentration (Chapalain, 1988; Boczar-Karakiewicz et al., 1988). In this procedure, the flow dynamics and the sediment concentrations are modelled separately. In pursuit of our goal consisting in studying heterogeneous sediment transport under wavetrains (i.e. in a two-dimensional configuration), a simple modelling which capture the main features of the flow is preferable to more complicated numerical solutions like this one mentioned above. To proceed in this way, we decide to test the capacity of a first-order decoupled model consisting in a constant (in time and space) effective eddy viscosity model.

The hydrodynamics of the wave-induced boundary layer flow is now described by an analytical approach using the following Reynolds averaged momentum equation

$$\frac{\partial u}{\partial t} + u \frac{\partial u}{\partial x} - \frac{\partial u}{\partial \eta} \int_0^\eta \frac{\partial u}{\partial x} d\eta = \frac{\partial U_b}{\partial t} + U_b \frac{\partial U_b}{\partial x} + \frac{1}{l^2} \left[ v_t \frac{\partial u}{\partial \eta} \right] \quad (16)$$

where  $\eta = z/l$  and  $l$  is a characteristic length scale of the boundary layer.

The required effective eddy-viscosity closure is obtained by applying following model

$$v_t = [U] \cdot [L] \quad (17)$$

where  $[U]$  and  $[L]$  are characteristic scales for the velocity and turbulent eddies respectively.

The velocity scale  $[U]$  is estimated by the friction velocity

$$u^* = \sqrt{\frac{\tau_{bm}}{\rho}} \quad (18)$$

where  $\tau_{bm}$  denotes the maximum bottom stress and the length scale  $[L]$  in (17) is assumed to be the ripple height (Nielsen et al., 1982).

A classical perturbation analysis provides explicit expressions for the first- and second-order horizontal mean velocity. Both expressions are defined in Appendix.

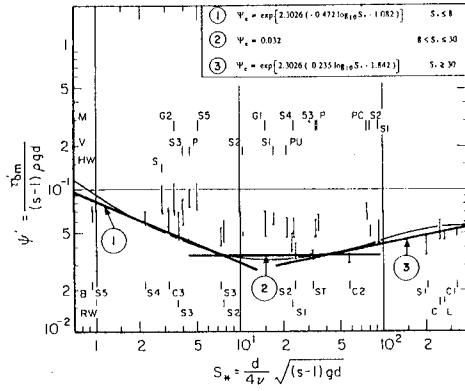


Figure 4. Madsen and Grant's wave extended Shields (1976) diagram.

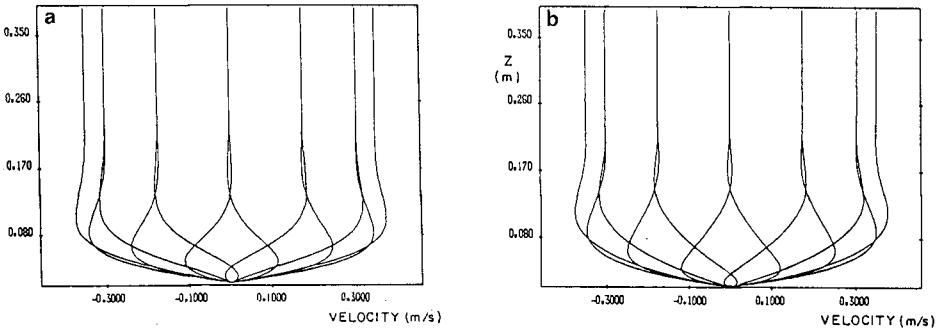


Figure 5. Mean velocity profiles calculated by the constant, time-independent eddy viscosity model [a], by the second-order turbulence closure model [b].

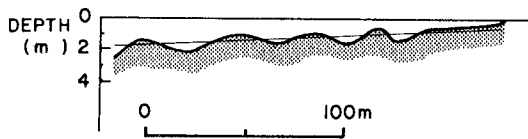


Figure 6. Observed bathymetric profile of Wasaga Beach.

The predicted velocity profiles for an oscillatory flow whose maximum velocity  $U_0$  and period are 0.35m/s and 10s respectively are shown in Figure 5 for every  $30^\circ$  of the wave-cycle. Comparison with results of the second-order turbulent closure model shows a satisfactory agreement.

A simple analytical model can now be derived for prediction of sediment concentration for each independent class in the wave-induced near-bed boundary layer flow.

The time-periodic and modally decomposed (Nielsen, 1979) sediment concentration  $c$ ,

$$c(K) = \sum_n^n c_n(K) \exp(in\omega t) \quad (19)$$

is assumed to satisfy the advective-diffusive equation (10) and the above boundary conditions.

Following the original solution of Nielsen (1979) the spatial and temporal sediment concentration is described by an explicit analytical expression  $c(K, X, z, t)$  (defined in the Appendix). In this expression the eddy diffusivity  $\gamma_t(K)$  is assumed proportional to the eddy viscosity  $\nu_t$  and dependent on the particle size according to Van de Graaff and Roelvink's (1984) relationship involving the fall velocity of the form

$$\gamma_t(K) = \frac{1}{1 + 23 \cdot w_f(K)} \quad (20)$$

### SEDIMENT TRANSPORT RATE AND RELATED SEABED RESPONSE

The wave-induced, time-averaged flux of sediment of class  $K$  is estimated by the product of the instantaneous sediment concentration and the sediment velocity vector

$$Q_J(K) = \frac{1}{T} \int_0^T \int_0^\delta u(X, z, t) c(K, X, z, t) dz dt \quad (21)$$

where subscript  $J$  denotes the box index resulting from the spatial discretization (i.e.  $X = J \Delta X$ )

In order to analyse the quantitative contributions of time-independent and time-dependent flow velocities and concentrations to the sediment flux  $Q$ , the product u.c. in (21) will be formally decomposed

$$u(X, z, t) \cdot c(X, z, t) = \left\{ \alpha u^{(1)}(X, z, t) + \alpha^2 \beta [u_s(X, z) + u_p^{(2)}(X, z, t)] \right\} \cdot [\bar{C}(X, z) + c(X, z, t)] \quad (22)$$

where  $u^{(1)}$  and  $u_p^{(2)}$  denotes the first and second-order periodic velocity components,  $u_s$  is the time-averaged velocity,  $\bar{C}$  denotes the mean concentration and  $c$  is the instantaneous concentration.

In the following we are separating the local sediment flux into two components

$$Q_J(K) = Q_{m_J}(K) + Q_{n_J}(K) \quad (23)$$

where  $Q_{m_J}(K)$  denotes the contribution of time-independent quantities and  $Q_{n_J}(K)$  the contribution of time-dependent quantities.

The component  $Q_{m_J}(K)$  is

$$Q_{m_J}(K) = \frac{S_J(K)}{T} \int_0^\delta \bar{C}(K, X, z) \cdot u_s(X, z) dz \quad (24)$$

where  $S_J(K)$  controls the threshold of sediment movement and defined by

$$S_J(K) = \begin{cases} 0 & \text{if } \psi'(K) < \psi'_c(K) \\ 1 & \text{if } \psi'(K) > \psi'_c(K) \end{cases} \quad (25)$$

Choosing now for the mean sediment concentration in (24) the following expression (Rouse, 1937)



$$\bar{C}(K, X, z) = \bar{C}_o(K, X) \exp(-D(K) z) \quad (26)$$

with  $D(K) = w_f(K) / \gamma_s(K)$

and substituting in (24) the mass transport velocity defined in Appendix, the component  $Q_{mj}(K)$  may also be expressed by an explicit formula given in Appendix.

Proceeding now in a similar way with time-dependant quantities in (22) the component  $Q_{nj}(K)$  may also be made explicit and the related expression is given in Appendix.

The "effective" sediment transport rate is obtained by weighting this latter quantity by the composition of the sediment substrate. Finally, the notion of "numerical" sediment rate is introduced for each class, such that

$$N_J^T(K) \simeq Q_J^T(K) \cdot P_J^T(K) / (4\pi r(K))^3 \quad (27)$$

The spatio-temporal evolution of the granulometric distributions is described by the continuity relation for each class of sediment. This procedure allows the calculation of the number of particles of each class present in the box J after exposure for a time  $\Delta T$  to the ambient hydrodynamic conditions, i.e.

$$N_J^{T+\Delta T}(K) = N_J^T(K) + (N_{J,f}^T(K) - N_{J+1}^T(K)) \quad (28)$$

The new updated local distribution for the different sediment classes is determined by

$$P_J^{T+\Delta T}(K) = \frac{N_J^{T+\Delta T}(K)}{\sum_{K=1}^{KM} N_J^{T+\Delta T}(K)} \quad (29)$$

The total instantaneous sediment transport rate is the sum of the individual transport rates corresponding to each class:

$$Q_J^T = \sum_{K=1}^{KM} Q_J^T(K) \quad (30)$$

The overall variation in depth is calculated using an equation of conservation of matter expressed in the form

$$h_J^{T+\Delta T} \simeq h_J^T - \Delta T \cdot [Q_{J-1}^T - Q_{J+1}^T] / (\Delta X \cdot C_p) \quad (31)$$

where  $C_p$  is the concentration of the compact bed arbitrary taken equal to 0.74 like for the idealized rhomboedric arrangement.

## APPLICATION

In order to contain the high costs of computation, the application of multicomponent modelling will be limited to the case of Wasage Beach located along the shore of Georgian Bay in Lake Huron. On account of its location in a narrow bay this area is hydrodynamically very well-controlled with waves whose period and height are respectively about 5s and 1m propagating exclusively from the north. The bathymetric profile illustrated in Figure 6 is characterized by a mean slope of 0.5% modulated by four bars. The granulometric analysis leads to consider a mean sediment grain diameter equal to 0.35mm. Even though local measurements of the granulometric distribution are not available on this profile, as an approximation one will apply here the synthetic results of Saylor and Hands (1970) pertaining to Great Lakes (Figure 1).

The initial granulometric curve has an average value of  $\bar{\phi}^0 = 1.5$  (corresponding to a sediment of mean diameter equal to 0.35 mm) and a root mean square deviation  $\sigma^0 = 0.5$ . The main parameters associated to this initial distribution are listed in Table 1.

In order to facilitate the comparison with the single class modelling, the results from the single class version will be placed beside those of the multiclass model.

The sediment transport rate distribution across the foreshore zone is shown in Figure 7-I. It displays slightly lower transport rates magnitude than for the single class case (Figure 7-II). The horizontal gradients are very close in both cases. For this reason, a very similar bathymetric response is obtained, generated on a characteristic time scale of the deformation that closely resembles that obtained in the single case version.

Figure 8 illustrates the spatial structure of the mean value and the root mean square deviation of the granulometric curve. Comparison of these results with the associated topography reveals:

(i) a drift of the the granulometric curve towards fine sediments at the crest and towards coarse sediments in the troughs (Figure 8a). The simulation is in agreement with the observations described in the introduction (Figures 1-2). Characteristic granulometric curves for crests and troughs are shown in Figure 9 (curves B and C, respectively).

(ii) degradation of the sorting at the crests combined with an improvement in the troughs (Figure 8b). This specific result is contradiction with all the observations, apart from some (outer zone) of those of Long et al. (1984) (Figure 2)

## CONCLUSION

Multicomponent simulation is an attempt to provide as realistic as possible a model for problems of sedimentation. From a quantitative point of view, this approach, although highly simplified, allows an appreciation of the impact of a fairly actual granulometric distribution on the transport of sediment across the foreshore profile. The global effect (i.e. on sediment transport rates and seabed response) proves insignificant on account of the crudeness of the modelling. The second, more novel, point which concerns the simulation of the spatial adjustment of the granulometric characteristics across the profile, shows that the model gives correct representation of what happens in nature as to the confinement of fine fractions at the crests of the bars and coarse fractions in the troughs between the bars. About the sorting of sediment classes, however, the model results are in contradiction with the main body of available in situ measurements. This discrepancy may suggest that there are many difficulties remaining and related to additional effects like for example wave breaking, reflected or trapped waves. Nevertheless, further effort to verify the basis of multiclass geomorphological modelling should be devoted to collect more data in laboratory and in the field in order to clarify the pattern of the sorting of sediment distributions across the bar systems.

## APPENDIX: WAVE-INDUCED VELOCITIES, SEDIMENT CONCENTRATION AND RELATED SEDIMENT TRANSPORT RATES IN THE NEAR-BED BOUNDARY LAYER

Substituting a perturbation series for  $u$

$$u = \alpha u^{(1)} + \alpha^2 u^{(2)} + \dots$$

into the Reynolds equation (16), the first-order oscillatory velocity component is

$$u = \alpha u^{(1)} = \alpha \operatorname{Re} \sum_{j=1}^2 U_j \exp[-(1+i)\eta_j] \quad (32)$$

$$\text{where } \eta_j = z/l_j = z / \sqrt{\frac{2\nu_t}{\omega_j}}$$

On account of the smallness of the imaginary part of the wave number  $k_j^I$  in geophysical conditions (Chapalain, 1988) the second-order steady velocity identified to the mass transport

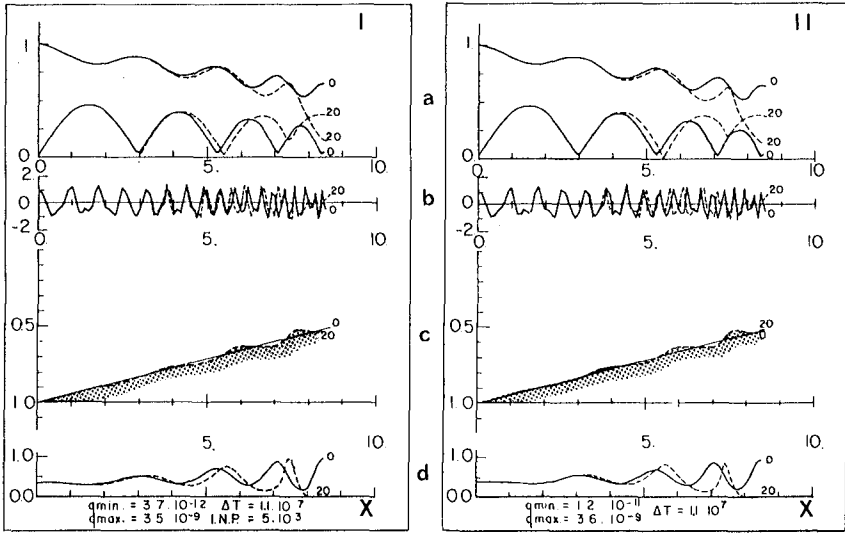


Figure 7. Multiclass model run (I) for Wasaga Beach, compared with single class model (II). (a) Two first harmonic component amplitudes non-dimensionalized by the wave amplitude. (b) Free surface elevation at a given time non-dimensionalized by the wave amplitude. (c) Near-shore topography non-dimensionalized by the incident water depth. (d) Total sediment transport rate  $Q$ . The horizontal distance  $X$  is measured in incident wavelengths.

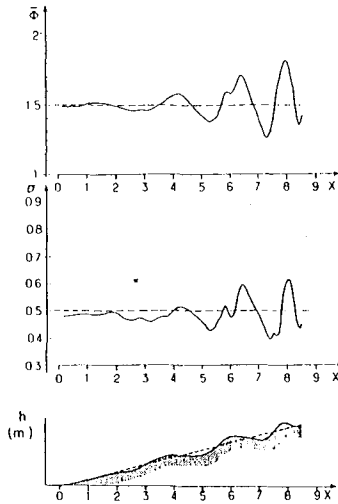


Figure 8. Calculated spatial structures of the mean value  $\bar{\phi}$  and of the sorting  $\sigma$  across Wasaga Beach foreshore profile.

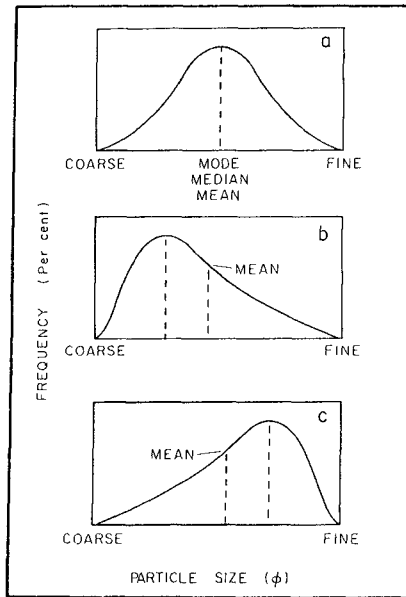


Figure 9. Typical granulometric distributions (A: initial normal distribution, B: characteristic distribution for troughs, C: characteristic distribution for the crests).

$\phi$ (K)	d (mm)	$W_f$ (m/s)	$\psi'_c$ (K)	$p^o$ (K)
-0.5	1.4	0.207	0.0367	0.00013383
0.0	1.0	0.153	0.0324	0.00443186
0.5	0.7	0.110	0.0320	0.05399113
1.0	0.5	0.0763	0.0320	0.24197145
1.5	0.35	0.0509	0.0338	0.39894347
2.0	0.25	0.0325	0.0432	0.24197145
2.5	0.177	0.0197	0.0552	0.05399113
3.0	0.125	0.01136	0.0705	0.00443186
3.5	0.088	0.00620	0.0901	0.00013383

Table 1. General Characteristics of sediment particles making up the multiclass substrate at Wasaga Beach in the numerical simulation.

velocity (Longuet-Higgins, 1953) may be approximated by

$$u_s = \frac{\alpha^2 \beta}{4} \sum_{j=1}^2 \left[ 1 - \frac{1}{6} \beta^2 k_j^R n^2 \right] \frac{\omega_j}{k_j^R} |a_j|^2 \exp\left(\frac{2k_j^I}{\beta}\right) H_j^I(\eta_j) \quad (33)$$

$$\text{where } H_j^I = -8 \exp(-\eta_j) \cos \eta_j + 3 \exp(-2\eta_j) + 5 \quad (34)$$

For convenience we omit to specify the sediment class index  $K$  in the following expressions. The expression for spatial and temporal evolution of the suspended sediment concentration is

$$c(X, z, t) = \sum_{n=1}^n \frac{\bar{C}_0}{1+\mu} \cdot \frac{a'_n}{\alpha_n} \left( \exp(-i n \Phi^+) + \mu \exp(-i n \Phi^-) \right) \exp\left(-\frac{w_f}{\gamma_t} \alpha_n z\right) \exp(in \omega_1 t) \quad (35)$$

$$\text{where } a'_n = \frac{2 (m!)^2}{(m+n)! (m-n)!}$$

$$\text{and } \alpha_n = \frac{1}{2} + \sqrt{\frac{1}{4} + i \frac{n \omega \gamma_t}{w_f}}$$

The time-independent sediment transport rate  $Q_m$  is

$$Q_m(X) = \frac{1}{4} \alpha^2 \beta \bar{C}_0(X) \sum_{j=1}^2 \frac{-8\delta_j}{(D\delta_j-1)^2 + 1} \left[ \exp(D\delta_j-1)\eta_{sj} \left( (D\delta_j-1) \cos \eta_{sj} + \sin \eta_{sj} \right) + 1 \right] \\ + \frac{3\delta_j}{D\delta_j-2} \exp[(D\delta_j-2)\eta_{sj}] + \frac{5}{D} \exp[-D\eta_{sj}] \quad (36)$$

The time-dependent sediment contribution  $Q_n$  in an integral form is

$$Q_n(X) = \frac{\delta}{2} \operatorname{Re} \left\{ \sum_{j=1}^2 \frac{\bar{C}_0}{(1+\mu) \alpha_j} U_j a'_j \left( \exp(-i j \Phi^+) + \mu \exp(-i j \Phi^-) \right) \int_0^\delta \exp\left(-\frac{w_f \alpha_j z}{\gamma_t}\right) (1 - \exp(-(1-i)\beta_j z)) dz \right\} \quad (37)$$

where  $\eta_{sj} = \delta/\delta_j$

This expression can be made explicit after some tedious algebra (Chapalain, 1988).

## REFERENCES

- Bajorunas, L. and Duane, D.B. (1967) Shifting offshore bars and harbor shoaling. *J. Geophys. Res.*, Vol 72, (24), 6195-6205.
- Boczar-Karakiewicz, B., Paplinska, B. and Winiecki, J. (1981) Formation of sandbars by surface waves in shallow water. Laboratory experiments. *Rozprawy Hydrotechniczne*, Vol 41, 11-25.
- Boczar-Karakiewicz, B., Bona, J.L. and Cohen, D.L. (1987) Interaction of shallow water wave and bottom topographies. in: *Dynamical Problems in Continuum Physics*. Springer Verlag, Vol.4, 131-176.
- Boczar-Karakiewicz, B., Chapalain, G. and Temperville A. (1988) Sand bars formation by waves in coastal zones. *Proc. of the 2nd International Symposium on Water Wave Research*, Hannover, 89-102.
- Boczar-Karakiewicz, B. and Davidson-Arnott, R.G.D (1988) Near-shore bar formation by non-linear wave processes-a comparison of model results and field data. *Marine Geology*, Vol.77, 287-304.

- Bowen, A.J. and Inman, D.L. (1971) Edge waves and crescentic bars. *J. Geophys. Res.*, Vol.76, 8662-8671.
- Carter, T.G., Liu, P.L.F. and Mei, C.C. (1973) Mass transport by waves and offshore sand bedforms. *J. Waterways, Harbour, Coastal Eng.*, Vol.99, 165-184.
- Chapalain, G. (1988) Etude hydrodynamique et sédimentaire des environnements littoraux dominés par la houle. Thèse de Doctorat de l'Université Joseph Fourier-Grenoble I.
- Davis, R.A. and McGreary, F.R. (1965) Stability in nearshore bottom topography and sediment distribution, southeastern lake Michigan. Pub. N° 13, Great Lakes Research Division. 222-231, 1965.
- Dyhr-Nielsen, M. and Sorensen, T. (1970) Some sand transport phenomena on coasts with bars. *Proc. of the 12th International Conference on Coastal Engineering*, 855-863.
- Forbes, D.L., Frobels, D., Heffler, D.E., Dickie K. and Shiels C. (1986) Surficial geology, sediment mobility, and transport processes in the coastal zone at two sites in the southern Gulf of St Lawrence: Pte Sapin (N.B.) and Stanhope Lane (P.E.I). C2S2 Report 20.
- Fox, W.T., Ladd, J.W. and Martin, M.K. (1966) A profile of the four moment measures perpendicular to a shore line, south haven, Michigan. *J. sedimentary Petrology*, Vol. 36, (4), 1126 - 1130.
- Gibbs, D., Matthews, M.D. and Link, D.A. (1971) The relationship between sphere size and settling velocity. *J. Sedimentary Petrology*, Vol.41, 1, 7-78.
- Graaff, J. van de and Roelvink, J.A., (1984) Grading effects in concentration measurements. *Proc. of the 19th Conference on Coastal Engineering*, 1618-1634.
- Grant, W.D. and Madsen, O.S. (1982) Movable bed roughness in unsteady oscillatory flow. *J. Geophys. Res.*, Vol. 87, C1, 469-481.
- Jonsson, I.G. (1978) A new approach to oscillatory rough turbulent boundary layers. Technical University of Denmark, Inst. of Hydrodynamics and Hydraulic Engineering. Ser. Pap. 17, p.87, 1978. (Also published in *Ocean Eng.*, 7, 109-152, 1980).
- Lau, J. and Barcelon V. (1972) Harmonic generation of shallow water waves over topography. *J. Phys. Oceanography*, 2, 405-410.
- Long, B.F., Boczar-Karakiewicz, B. and Drapeau, G. (1984) Transport sédimentaire dans un système de barres d'avant-côte. Abstract book, C0411, 27ème International Geology Congress, Moscow.
- Longuet-Higgins, M.S. (1953) Mass transport in water waves. *Phil. Trans. Roy. Soc. Lond.*, A, 245, 535-591.
- Madsen, O.S. and Grant, W.D. (1976) Quantitative description of sediment transport by waves. *Proc. of the 19th Conference on Coastal Engineering*, 1093-1112.
- Mothersill, J.S. (1969) A grain size analysis of longshore - bars throughs , lake superior, Ontario. *J. Sedimentary Petrology*, Vol. 39, (4), 1317-1324.
- Nielsen, P. (1979) Some basic concepts of wave sediment transport. Technical University of Denmark, Inst. of Hydrodynamics and Hydraulic Engineering, Ser. Pap. 20, p. 160.
- Nielsen, P., Green, M.O. and Coffey, F.C. (1982) Suspended sediment under waves. Coastal Studies Unit Technical Report 82/6.
- Rouse, H. (1937) Modern concepts of mechanics of turbulence. *Trans. Am. Soc. Civ. Eng.*, Vol.102, 463-543.
- Saylor, J.H. and Hands, E.B. (1970) Properties of lonshore bars in the Great Lakes. *Proc. of the 12th International Conference on Coastal Engineering*, 839-853.
- Sheng, Y.P. and Villaret, C. (1989) Modeling the effects of suspended sediment stratification on bottom exchange processes. *J. Geophys. Res.*, Vol.94, C10, 14429-14444.
- Sitarz, J.A. (1963) Contribution à l'étude de l'évolution des plages à partir de la connaissance des profils d'équilibre. Travaux du C.R.E.O., Tome V, Fasc. II, III, IV.
- Svendsen, I.A. (1977) A model of sediment motion under waves. Internal Research Note, Technical University of Denmark, Inst. of Hydrodynamics and Hydraulic Engineering.